

Blood phantom verification of a new compact DOT system

Bertan Hallacoglu¹, Jason W. Trobaugh^{1,2}, Kate L. Bechtel³, Chandran V. Seshagiri¹

¹Cephalogics, 33 Arch St. Suite 320, Boston, MA 02110

²Department of Electrical and Systems Engineering, Washington University in St. Louis, MO 63110

³Triple Ring Technologies, Newark, CA 94560

Author e-mail address: bertan.hallacoglu@cephalogics.com

Abstract: We have developed a compact high-density DOT system for cerebral oxygenation and perfusion imaging on the bedside and demonstrated its insensitivity to the superficial layer in a custom two-layered blood phantom.

OCIS codes: (110.0113) Imaging through Turbid Media; (110.6955) Imaging systems; (120.3890) Medical Optics Instrumentation

1. Introduction

Patients with a variety of neural disease states including cerebral hemorrhage, ischemia, and head trauma are at risk of impaired cerebral perfusion. Reliable, accurate, continuous, bedside imaging of cerebral tissue oxygen saturation (StO₂) could help clinicians manage perfusion in these patients. However, demonstrating the accuracy and performance of StO₂ measurements *in vivo* remains challenging since no reference standard exists.

Measurements in tissue-mimicking phantoms provide a reasonable first-step towards verification of system performance and characterization. Intralipid (IL) and ink phantoms have been commonly used to verify measurements of optical properties; blood phantoms have been used to better mimic physiology and incorporate physiologically relevant absorption and scattering spectra; other phantom experiments have included multi-layer designs to approximate the layered composition of the human head. Combining these ideas, we have designed a two-layered blood phantom for verification of blood oxygen saturation (SO₂) measurements in the “brain” layer. In this abstract, we report preliminary measurements on this phantom using a compact, high-density diffuse optical tomography (DOT) system that we have developed for cerebral perfusion imaging on the bedside.

2. Materials and Methods

The DOT system used for these measurements provides a high-density arrangement of 10 source optodes and 18 detector optodes printed on rigid-flex circuit boards for flexibility (Fig.1a). Each source optode contains five time-encoded, amplitude-modulated Vertical Cavity Surface Emitting Lasers (VCSELs) operating at five different wavelengths ranging from 690-850nm. Each detector optode contains a single photodiode with a synchronous detection design that collects overlapping, continuous-wave measurements across source-detector distances ranging from 13-87mm over 9 nearest-neighbors. The system acquires measurements from 180 channels per wavelength at a 5Hz frame rate. Acquired data is digitized, processed, and transmitted to a laptop via Ethernet connection for post-processing. The acquisition system has a dynamic range of over 10⁷, or 140dB.

A custom phantom enclosure was constructed with dimensions of 120x60x45mm and sealed to provide watertightness. A custom built front wall for the enclosure was developed with cutouts to house the DOT sensor-array. Optical windows for emission and detection of optical intensities were made of ~0.1mm thick Lexan polycarbonate film (refractive index ~1.6). Slits were incorporated 15mm from the front wall for placement of a translucent separator to create two separated layers (Fig.1b). As guided propagation has been shown to affect similar liquid-phantom setups [1], we tested several diffusers with different coatings to identify the separator material that introduced the smallest perturbation of the detected optical intensities. The materials tested included C-HE05-S-M, C-HE10-S-M, C-HH80, C-HH20 (Brightview Technologies, Durham, NC). All materials had thickness of 0.178mm with refractive index ~1.46, which is similar to that of IL in water (~1.33). The phantom enclosure was filled with an IL+water solution and candidate diffuser materials were tested based on optical intensities recorded before and after placing the diffuser. At the furthest source-detector separation considered in the data analysis (53.6mm) the absolute % deviation was below 6% for all four diffusers. C-HH20 was determined to be the least intrusive with absolute % deviation of only ~0.4%, and this material was used as the separator for all subsequent measurements.

IL 20% (Sigma Aldrich, St. Louis, MO), water, and fresh bovine blood were mixed to create suspensions with reduced scattering coefficients and fraction of blood-to-tissue (blood-to-IL) volume representative of brain tissue. Typical mixtures used by volume were 6% IL to water (resulting in $\mu'_s \sim 10\text{cm}^{-1}$ at 800nm), and 3.5% blood to IL+water. In the first experiment, layer 2 of the phantom was desaturated by the addition of yeast and sugar [2]. In a separate experiment, layer 1 was desaturated to assess sensitivity of the analysis to superficial changes. DOT measurements were acquired continuously through the front wall of the phantom enclosure for ~10 mins prior to the addition of the yeast (baseline) and for 30-40 mins following the addition of the yeast. Oxygen tension (PO₂) and temperature of the

desaturated layer were recorded (Neofox, Ocean Optics, Dunedin, FL) away from the DOT sensor-array and converted to SO_2 using the hemoglobin disassociation curve to serve as a reference. The DOT system and experimental setup are shown in Fig.1.

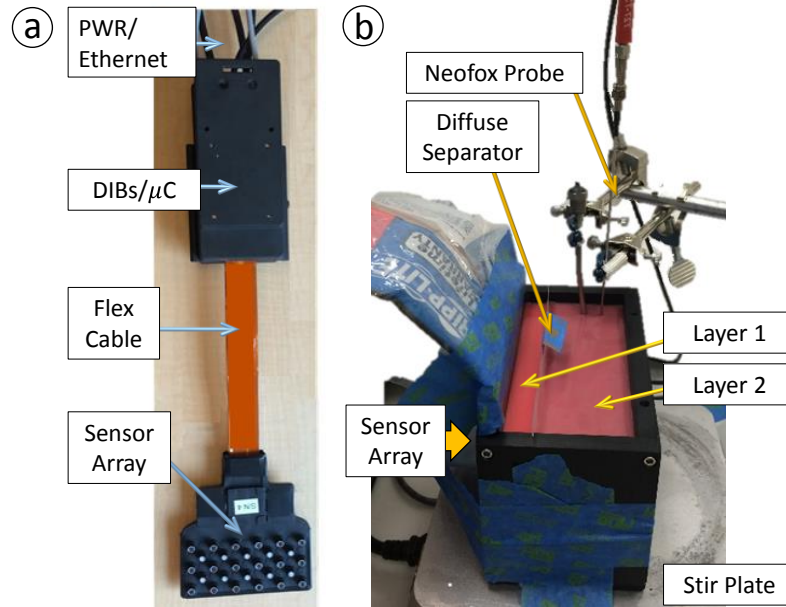


Fig.1. Illustration of (a) the DOT System made of a compact sensor-array, digital interface boards/microcontroller enclosure (DIBs/μC), and a flex cable; and (b) two-layer blood phantom setup, showing the placement of the DOT sensor-array and the PO_2 /temperature probes during measurements

To estimate the 2nd layer SO_2 , the linear Rytov approximation, expressed as $y = Ax$, was used to relate measured light intensities to perturbations of oxy- (HbO) and deoxy-hemoglobin (HbR) from a background model. Here, $y = -\log(\phi/\phi_0)$ is a vector of ratios of measured light intensities (ϕ) to a two-layer diffusion model (ϕ_0 , the background), and x is a voxelized representation of HbO and HbR perturbation images. The matrix A was constructed from sensitivity matrices for each wavelength, constructed for our DOT optode geometry as in [5], and corresponding hemoglobin extinction coefficients. The Green's function solutions for a two-layer slab model were obtained using NIRFAST [3] to solve the finite-element forward model. Background μ'_s and chromophore concentrations were determined by fitting the data sequentially with a homogenous diffusion model followed by a two-layer diffusion model [4], resulting in background optical intensity, ϕ_0 . Directly solving for chromophore concentrations, as opposed to first determining absorption coefficients, leverages multi-wavelength information, reduces unknowns, and constrains the inverse problem. Perturbation images of HbO and HbR were estimated using depth-dependent Tikhonov regularization and a Moore-Penrose generalized inverse [5]. Evaluated hemoglobin perturbations for each frame were added back to background values to evaluate SO_2 . Measurements were processed into 2-D images of layer 2 and image means were compared to reference SO_2 values.

3. Results

In both experiments, addition of yeast led to marked reductions in measured SO_2 from 100% to as low as ~5%. DOT results for layer 2 desaturation are highlighted in Fig 2, where means of SO_2 images of layer 2 are displayed on the bottom panel for comparison with the reference SO_2 measurement. Absence of noticeable edge effects in the images confirms semi-infinite boundary assumption, and spatial uniformity of the images with low coefficient of variation ($\text{CV} < 0.03$ across all images) indicates uniform desaturation in layer 2. Some discrepancy between the two temporal curves is expected considering differences in the physical positioning of the DOT sensor-array and the PO_2 probe in the phantom as well as in units of measurement. While the usage of hemoglobin disassociation curve for PO_2 to SO_2 conversion should be applicable *ex vivo*, the accuracy of this approach needs to be validated against a more direct measure such as gas analysis.

Desaturation in layer 1 did not reduce SO_2 measurements of layer 2 (Fig. 3), which is an important demonstration of the algorithm's relative insensitivity to changes in the superficial layer. SO_2 above 100% in the latter portion of the experiment indicates inaccuracies for small values of HbR.

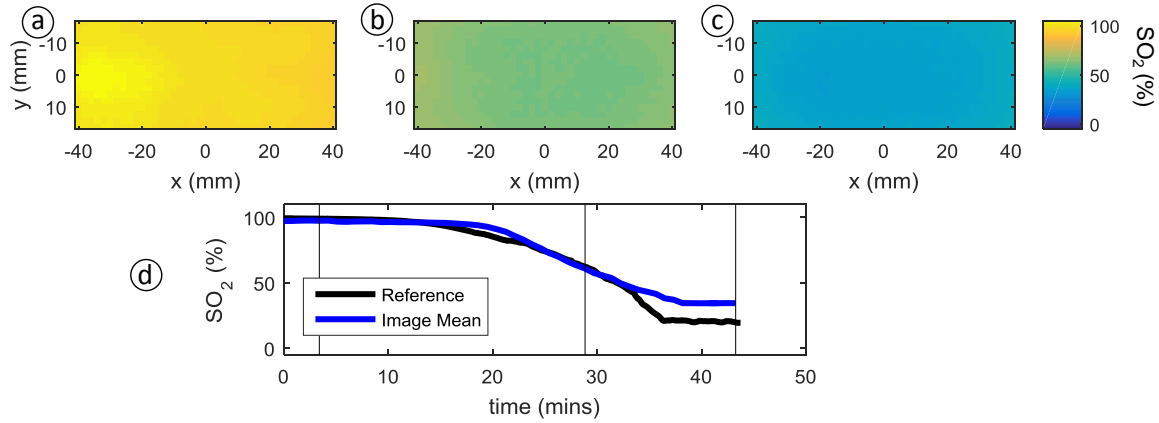


Fig. 2. Results of layer 2 desaturation experiment. SO₂ images of layer 2 at discrete time points (a)-(c); and comparison of temporally plotted mean±stdev of images of layer 2 (blue line) with the reference measurement (black line). Mean±stdev was comparable to thickness of the line. Discrete time points of the images are indicated by the vertical lines in (d).

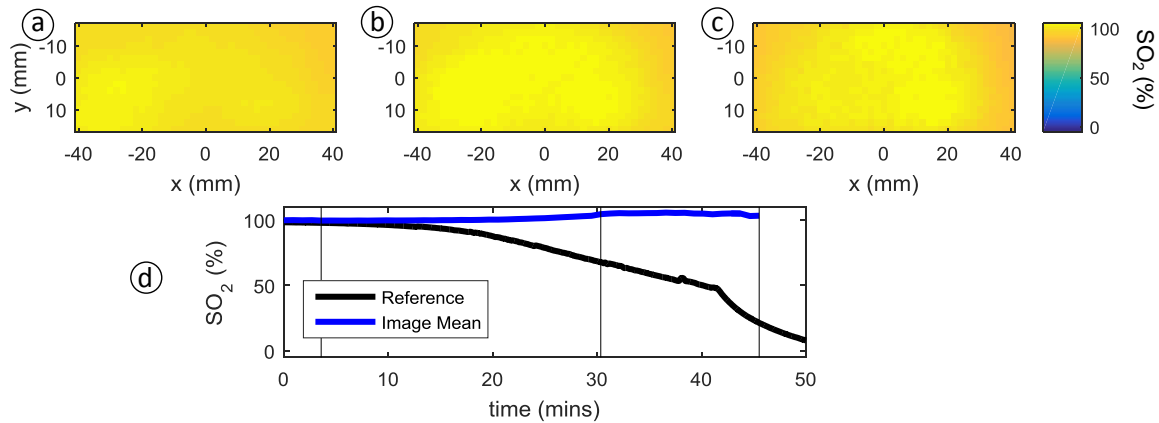


Fig. 3. Results of layer 1 desaturation experiment. SO₂ images of layer 2 at discrete time points (a)-(c); and comparison of temporally plotted mean±stdev of images of layer 2 (blue line) with the reference measurement in layer 1 (black line). Mean±stdev was comparable to thickness of the line. Discrete time points of the images are indicated by the vertical lines in (d).

4. Conclusion

These results demonstrate the feasibility of using a layered blood phantom design to test the SO₂ imaging capability of a new DOT system. We have demonstrated the sensitivity of our approach to SO₂ values beneath a thickness representative of typical scalp-to-cortex distance while remaining insensitive to SO₂ changes in that thickness. We are currently exploring alternative arrangements for the diffuse separator to create spatial SO₂ differences in the imaging field. These are important steps towards developing validation protocols in the absence of an accepted reference standard for cerebral StO₂ imaging.

References

- [1] S. Del Bianco, F. Martelli, F. Cignini, G. Zaccanti, a Pifferi, a Torricelli, a Bassi, P. Taroni, and R. Cubeddu, "Liquid phantom for investigating light propagation through layered diffusive media.," *Opt. Express*, vol. 12, no. 10, pp. 2102–2111, 2004.
- [2] S. Suzuki, S. Takasaki, T. Ozaki, and Y. Kobayashi, "A tissue oxygenation monitor using NIR spatially resolved spectroscopy," *Proc. SPIE*, vol. 3597, no. January 1999, pp. 582–592, 1999.
- [3] H. Dehghani, M. E. Eames, P. K. Yalavarthy, S. C. Davis, S. Srinivasan, C. M. Carpenter, B. W. Pogue, and K. D. Paulsen, "Near infrared optical tomography using NIRFAST: Algorithm for numerical model and image reconstruction," *Commun. Numer. Methods Eng.*, vol. 25, pp. 711–732, 2009.
- [4] A. Liemert and A. Kienle, "Light diffusion in N-layered turbid media: steady-state domain.," *J. Biomed. Opt.*, vol. 15, no. 2, p. 025003, 2010.
- [5] J. P. Culver, T. Durduran, D. Furuya, C. Cheung, J. H. Greenberg, and a G. Yodh, "Diffuse optical tomography of cerebral blood flow, oxygenation, and metabolism in rat during focal ischemia.," *J. Cereb. Blood Flow Metab.*, vol. 23, no. 8, pp. 911–924, 2003.